10.1109/ULTSYM.2013.0311

Spatial-resolution optimization of 3D high-frequency quantitative ultrasound methods to detect metastatic regions in human lymph nodes

Jonathan Mamou*†, Emi Saegusa-Beecroft‖, Alain Coron‡§, Michael L. Oelze#, Tadashi Yamaguchi<, Masaki Hata‖, Eugene Yanagihara‖, Junji Machi‖, Pascal Laugier‡§, and Ernest J. Feleppa†
†Frederic L. Lizzi Center for Biomedical Engineering, Riverside Research, New York, NY, USA
‖University of Hawaii and Kuakini Medical Center, Honolulu, HI, USA
‡CNRS, UMR 7623, Laboratoire d'Imagerie Paramétrique, F-75006, Paris, France
§UPMC Univ Paris 06, UMR 7623, LIP, F-75005, Paris, France
#Bioacoustics Research Laboratory, University of Illinois, Urbana, IL, USA
<Research Center for Frontier Medical Engineering, Chiba University, Chiba, Japan
*E-mail: jmamou@riversideresearch.org

***Abstract*—Proper staging and treatment of cancer require accurate detection of lymph-node metastases, but current histological methods fail to detect small, but clinically significant metastases. We used novel 3D quantitative ultrasound (QUS) methods to identify metastatic regions in freshly excised lymph nodes from cancer patients. Individual lymph nodes were scanned in 3D using a 26-MHz, single-element, F2 transducer with a 12-mm focal length. QUS methods quantified the backscatter coefficient to yield four estimates in cylindrical regions of interest (ROIs) having equal lengths and diameters ranging from 0.4 to 1 mm. To optimize the tradeoff between QUS-estimate quality and the spatial resolution of the estimates, the effect of ROI size on estimate bias and variance was investigated using a database of 101 lymph nodes of colorectal-cancer patients. Estimates were combined using linear-discriminant approaches and ROC curves were computed to assess classification performance. A Bayesian approach was used to convert the discriminant scores to 3D cancer-probability estimates throughout each lymph node. Analysis indicated that ROIs with a 0.8-mm length and diameter improved spatial resolution and minimally degraded estimate quality with an average variance increase of $<$20% for each estimate. The area under the ROC curve remained greater than 0.92 for all ROI sizes. Our QUS methods potentially can reduce the rate of false-negative determinations drastically by efficiently guiding pathologists to suspicious regions in lymph nodes, and having the best possible spatial resolution while retaining adequate estimate quality is critical.**

***Index Terms*—high-frequency ultrasound, quantitative ultrasound, lymph node, metastasis.**

I. Introduction

Detection of small metastatic regions (i.e., micrometastases) in excised human lymph nodes is critical to proper staging, patient management, and treatment planning. A cancer is termed node-positive when a lymph node contains at least one metastatic region larger than 200 μm. Typical lymph nodes have sizes ranging from 3 mm to more than 2 cm, and current standard-of-care histology protocols suffer from time and cost constraints that lead to an unacceptable rate of false-negative determinations [1], [2].

In an ongoing project, we have investigated the ability of a wide range of three-dimensional (3D) high-frequency quantitative ultrasound (QUS) methods to detect cancerous regions within excised lymph nodes obtained from histologically-proven cancer patients [3]–[5]. These QUS methods infer information about tissue properties from the backscattered radio-frequency (RF) echo signals. To perform our lymph-node QUS studies, a custom-made, high-frequency, ultrasound scanning system using a 26-MHz single-element transducer was developed and used to acquire 3D RF ultrasound data from individual lymph nodes that were excised for histological evaluation and staging according to standard medical practice. In addition, for this study, histology thin sections were acquired every 50 μm to guarantee that no clinically significant metastatic regions would be missed.

QUS methods based on the backscatter coefficients are stochastic in nature, and they rely on processing several adjacent RF segments, or regions of interests (ROIs), to yield statistically stable QUS estimates. Therefore, when statistical stability is a primary concern, and adequate microstructural tissue homogeneity can be assumed, large ROIs are preferred, and as a result, the spatial resolution of images that depict QUS estimates is coarser than that of the equivalent conventional ultrasound images. In our lymph-node studies to date, we used 3D cylindrical ROIs having a fixed length of 1 mm (along the transducer axis) and a diameter of 1 mm (transverse to the transducer axis).

In this paper, we experimentally investigate the tradeoff between robust, statistically stable QUS estimates and QUS-image spatial resolution. The goal of this study was to provide experimental guidance in choosing an appropriate ROI size for clinical application of these methods because the long-term goal of this project is to guide pathologists efficiently towards suspicious regions in lymph nodes. To this end, we used a database of 101 lymph nodes obtained from 46 patients diagnosed with colorectal cancer. This representative data set

included 18 nodes that were almost entirely filled with cancer and 83 that were entirely devoid of cancer. We refer to this set of lymph nodes as the uniform lymph-node database. These nodes were processed using a wide range of 3D ROI sizes. In addition, the study was limited to the four QUS estimates that quantified the ultrasound backscatter coefficient.

II. Methods

A. Ultrasound data acquisition and histology processing

Lymph-node dissection, histologic preparation, and ultrasound data-acquisition protocols have been described for this study [3]. Lymph nodes were obtained from patients with histologically-proven colorectal cancers at the Kuakini Medical Center (KMC) in Honolulu, HI. Following surgical excision, lymph nodes were brought to the pathologist for gross preparation. Then, individual nodes were placed in a water bath containing isotonic saline (0.9% sodium chloride solution) at room temperature and ultrasonically scanned in 3D by raster scanning over the lymph node. Adjacent scan lines and planes were uniformly spaced every 25 μm over the entire lymph node. Scanning was performed using a focused, single-element transducer (PI30-2-R0.50IN, Olympus NDT, Waltham, MA) that had a diameter of 6.1 mm, a focal length of 12.2 mm, a center frequency of 25.6 MHz, and a -6-dB bandwidth that extended from 16.4 to 33.6 MHz. The theoretically predicted pulse length in tissue and a 6-dB beam width of the HFU imaging system were 86 and 116 μm, respectively. The transducer was excited by a Panametrics 5900 pulser/receiver (Olympus NDT, Waltham, MA), and the RF echo signals were digitized at 400 MS/s using an 8-bit Acqiris DB-105 A/D board (Acqiris, Monroe, NY).

The Institutional Review Boards (IRBs) of the University of Hawaii and the KMC approved the participation of human subjects in the study. All participants were recruited at KMC and gave written informed consent, as required by both IRBs.

B. Backscatter quantification

To quantify backscatter, two distinct, ultrasound-scattering models were used; both employed fits to attenuation-compensated, normalized spectra obtained for each ROI. The first scattering model used a Gaussian form factor and yielded two QUS estimates: effective scatterer size, D, and effective acoustic concentration, CQ^2. For simplicity, this scattering model is termed the Gaussian model. The second scattering model was based on a linear-regression approximation to the normalized spectrum; it yielded two QUS estimates: spectral intercept, I, and spectral slope, S. This model is termed the straight-line model. The methods used to obtain the normalized spectra, to compensate for attenuation, and to fit the two scattering models, have been described in detail [3].

C. ROI size and step size

In this project to date, the "standard" ROI has been a 3D cylinder with a length of 1 mm and a diameter of 1 mm. In this paper, we consider this ROI size to be the reference for comparison to smaller ROI sizes and for assessing the tradeoff between spatial resolution and estimate quality. Table I displays the sizes of the ROIs under investigation. In addition, the spacing between adjacent ROIs was kept at half the size of the ROI (i.e., two adjacent ROIs have about 50% overlap). This spacing is equal to the QUS voxel size as shown in Fig. 3 of Ref. [3].

TABLE I: Properties of ROIs inder investigation

Name	Length (mm)	Diameter (mm)	Number of independent resolution cells	Percentage of $R_{1,1}$ volume
$R_{1,1}$	1	1	864	100%
$R_{0.9,0.9}$	0.90	0.90	630	72.9%
$R_{0.8,0.8}$	0.80	0.80	442	51.2%
$R_{0.7,0.7}$	0.70	0.70	296	34.3%
$R_{0.6,0.6}$	0.60	0.60	187	21.6%
$R_{0.5,0.5}$	0.50	0.50	108	12.5%
$R_{0.4,0.4}$	0.40	0.40	55	6.4%

Table I also introduces notations used to refer to each ROI size in this paper: the notation $ROI_{L,D}$ means an ROI of length L and diameter D in mm. This notation encompasses all cases studied because only cylindrical ROIs were considered. Following this notation, the standard ROI is denoted by $ROI_{1,1}$. From the ultrasound beam and pulse properties, the theoretical 3D resolution cell of the ultrasound imaging system, V_r, can be estimated to be a cylinder of length 86 μm and diameter 116 μm; therefore, $V_r = \pi * (116/2)^2 * 86 = 9.01 * 10^{-4}$ mm^3. Theoretical and experimental studies have shown that the standard deviation and bias of QUS estimates decrease as the number of independent resolution cells included in the ROI increases [6]. Therefore, the number of independent resolution cells for each ROI size also is shown in the last column of Table I.

D. Statistical analysis and classification performance

To investigate the effect of the ROI size on the quality of the four QUS estimates, we computed the mean values and standard deviations of each QUS estimate over each lymph node. Then, to assess the effect of reducing the ROI size when compared to our standard ROI size, we investigated the mean ratio of the standard deviation (MRS) of each QUS estimate to the standard deviation obtained for the standard ROI. Thus, four Student t tests were then performed to determine whether each average ratio (computed from the 101 lymph nodes) were statistically different (with α=0.05) from 1 because an MRS of approximately 1 would be expected if the ROI size had no significant effects on the QUS estimates.

In addition, for each of the two scattering models, the two corresponding QUS estimates were linearly combined to develop a linear classifier. Specifically, the average values of the two QUS estimates for each uniform lymph node were computed and a linear-discriminant function, Δ, was computed using the Fisher linear-discriminant approach, which maximizes the ratio of the interclass variance to intraclass variance. The linear-discriminant approach was used to evaluate the classification performance of each scattering model as a function of the ROI size. The classification performance was evaluated by deriving ROC curves and computing the area

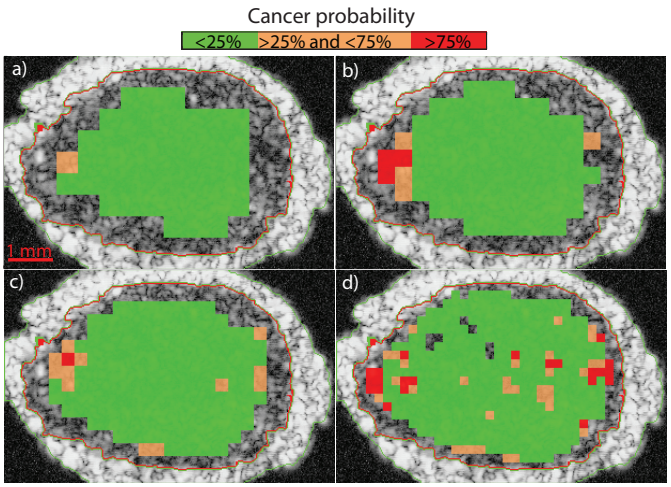

Fig. 1: Representative cancer probability QUS images of a non-cancerous lymph node as a function of ROI size: a) 1-mm length and diameter, b) 0.8-mm length and diameter, c) 0.6-mm length and diameter, and d) 0.4-mm length and diameter.

TABLE II: Mean of ratios of standard deviations (MRS) for each QUS estimate. Reference size is $R_{1,1}$.

	Gaussian model		Straight-line model	
ROI size	MRS(D)	MRS(CQ^2)	MRS(I)	MRS(S)
$R_{0.9,0.9}$	1.19±0.16	1.13±0.15	1.12±0.12	1.12±0.14
$R_{0.8,0.8}$	1.20±0.19	1.21±0.17	1.21±0.17	1.19±0.19
$R_{0.7,0.7}$	1.33±0.27	1.32±0.27	1.33±0.21	1.36±0.26
$R_{0.6,0.6}$	1.59±0.34	1.55±0.40	1.50±0.28	1.51±0.34
$R_{0.5,0.5}$	1.83±0.43	1.86±0.55	1.67±0.35	1.71±0.42
$R_{0.4,0.4}$	2.05±0.54	2.22±0.72	1.91±0.46	1.95±0.55

TABLE III: Classification performance achieved using each scattering model as a function of ROI size. The coordinates of a clinically-relevant operating point are also included.

	Gaussian model			Straight-line model		
ROI size	AUC	Sens.(%)	Spec. (%)	AUC	Sens. (%)	Spec. (%)
$R_{1,1}$	0.953±0.026	94.4	84.5	0.927±0.038	90.5	77.8
$R_{0.9,0.9}$	0.960±0.021	95.0	79.2	0.939±0.032	92.7	75.0
$R_{0.8,0.8}$	0.953±0.022	95.2	78.5	0.933±0.032	92.5	76.2
$R_{0.7,0.7}$	0.960±0.019	95.2	76.8	0.939±0.031	92.9	76.2
$R_{0.6,0.6}$	0.969±0.016	95.2	82.2	0.951±0.024	93.8	81.0
$R_{0.5,0.5}$	0.970±0.017	95.2	87.5	0.960±0.021	91.1	85.7
$R_{0.4,0.4}$	0.973±0.015	95.2	88.3	0.963±0.019	93.7	85.7

under the ROC (AUC) for both scattering models and each ROI size. Finally, Δ was used to compute an *a posteriori* cancer probability, P, for each ROI of each lymph node using a previously described Bayesian approach [7].

III. Results

A. Representative lymph node

To illustrate how the ROI size influences the QUS estimates, Fig. 1 displays one cross-sectional QUS-based cancer-probability image of a cancer-free lymph node for four distinct ROI sizes. Visual inspection of the QUS images indicates that as the ROI size decreases, the cancer probability estimates depict a greater degree of variation between adjacent ROIs. In addition, the proportion of ambiguous (i.e., cancer-probability between 25% and 75%) and false-positive ROIs (i.e., cancer probability greater than 75%) increases as the ROI size reduces. This means that the range of cancer-probability estimates becomes wider and less reliable because this lymph is entirely non-cancerous. Finally, Fig. 1d shows ROIs without any cancer-probability estimates (i.e., "holes" appear in the QUS image). This occurs when the QUS estimation breaks down or returns unrealistic estimates.

B. Statistical study for each QUS estimate

MRS values were computed for each of the four QUS estimates (Table II) using the uniform lymph-node database. As expected, the MRS value increases for all four QUS estimates as the ROI size decreases. In addition, MRS values all failed the t-test for any of the four QUS estimates. This means that the ROI size, in fact, does have an effect on the standard deviation of the estimates.

Finally, Table II also provides important information for choosing ROI size for a potential clinical application: using $R_{0.8,0.8}$ or $R_{0.7,0.7}$ possibly could provide greatly improved spatial resolution (e.g., by a factor of 2 or 3) in QUS images with only a small decrease in the robustness of QUS estimates (e.g., increase in variance of 20 or 30%). For specific cases where spatial resolution would be critical in the QUS image, $R_{0.6,0.6}$ potentially could be used while keeping in mind the cost in terms of a decrease in QUS-estimate quality. However, Table II strongly indicates that $R_{0.5,0.5}$ and $R_{0.4,0.4}$ should be avoided.

C. Database study

The next step of the study used the uniform lymph-node database to develop linear classifiers and assess their classification performance based on relative ROC-curve AUC values as shown in Table III. The AUC values shown in Table III range from 0.927 to 0.973 which demonstrate excellent classification independent of the scattering model or ROI size. Table III also displays coordinates of a possible clinically-relevant operating point (i.e., high sensitivity). Clinicians prefer to not miss cancers (i.e., they prefer a low rate of false-negative determinations) at the expense of a slight increase rate of false-positive determinations. As expected because of the AUC values, all quoted operating points display high to very high sensitivity with a corresponding specificity of at least 75%. However, while Table III demonstrates that the uniform lymph-node database can be used to produce satisfactory classifiers with any ROI size, it does not indicate that any ROI size can be used to perform classification; this was illustrated in Fig. 1.

Finally, to further analyze the ROI size effect on local classification performance, another study was conducted. In this study, individual ROIs were selected in each lymph node and for each ROI size and used to obtain ROC curves. Specifically, 10 ROIs were randomly selected from each lymph node of the database for $ROI_{1,1}$. Then, as the ROI size decreased, the number of randomly selected ROIs increased

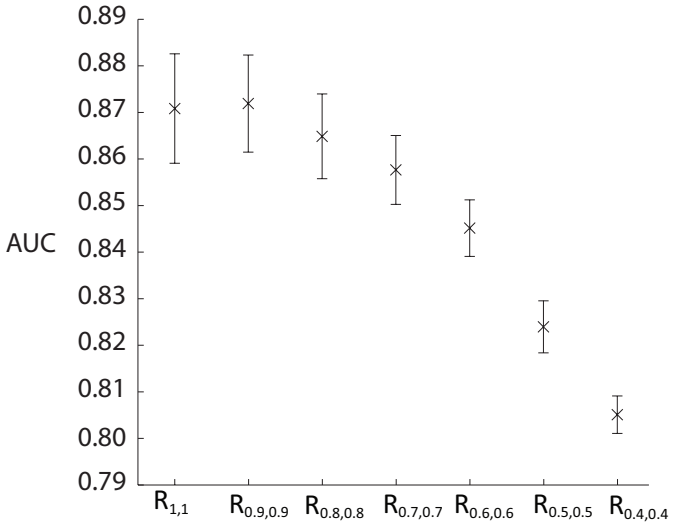

Fig. 2: Area under the ROC curve obtained using randomly-selected ROIs from each lymph node of the database as a function of ROI size; to obtain mean and standard deviation values, the random selection process was performed 250 times.

so that the same volume was randomly sampled from each node independent of the ROI size. This sampled volume per lymph node was equal to 7.85 mm^3, which was equal to about the third of the volume of the smallest lymph node in the database. To obtain mean and standard deviations values of the AUC, this random selection process was repeated 250 times for each ROI size. Figure 2 demonstrates that as the ROI size diminished the classification performance worsens with AUC values dropping from above 0.87 to below 0.81. The results show very similar AUC values for $ROI_{1,1}$, and $ROI_{0.9,0.9}$ (paired t-tests failed to find the mean AUC values to be statistically different at $\alpha = 0.05$). This demonstrates that using a slightly smaller ROI size did not degrade the results. The AUC values decreased with ROI volume for ROIs smaller than $ROI_{0.9,0.9}$ (paired t-tests found every other paired AUC value to be significantly different). Nevertheless, AUC values remain satisfactory for $ROI_{0.8,0.8}$ (i.e., 0.865) and arguably satisfactory for $ROI_{0.7,0.7}$ (i.e., 0.858), but degrade quickly for smaller ROI sizes.

IV. Conclusions and perspectives

The potential ability of our QUS methods to guide pathologists towards suspicious regions in lymph nodes is of great clinical value because it could drastically reduce the current unacceptably high rate of false-negative determinations. The 3D QUS methods we have developed show great promise for achieving this potential. In particular, we have been able to obtain near-perfect classification of lymph nodes that either were completely metastatic or completely devoid of metastases using only two QUS estimates based on Gaussian or straight-line models. However, these QUS methods use ROIs to compute QUS estimates because they are designed to provide estimates of stochastic properties of backscattered RF ultrasound signals. Therefore, QUS images have a much poorer spatial resolution than is available in the original ultrasound data. In this study, we evaluated the effect of reducing ROI size on QUS estimates using experimental but well-controlled data obtained from a large database of lymph nodes excised from histologically-proven cancer patients. Having the best possible QUS spatial resolution is invaluable for lymph nodes that are partially metastatic and contain small, but clinically-significant metastatic foci. This study provided strong evidence that the standard ROI size (i.e., $R_{1,1}$) was conservative and provided amply reliable QUS estimates. More important, this study demonstrated that $R_{0.8,0.8}$ is nearly as good as $R_{1,1}$ and could be used with very limited effect on the quality of QUS estimates while significantly improving QUS-image spatial resolution because $R_{0.8,0.8}$ has approximately half the volume of $R_{1,1}$ (Table I). Results also clearly indicated that $R_{0.4,0.4}$ and $R_{0.5,0.5}$ should not be used as they yield QUS estimates of very poor quality and AUC values below 0.83 when using randomly-selected ROIs). Finally, $R_{0.7,0.7}$ and $R_{0.6,0.6}$ are somewhat intermediate cases that could be used "with caution" under certain conditions that require fine spatial resolution at the cost of poorer QUS-estimate quality.

ACKNOWLEDGEMENTS

This research was supported in part by NIH Grant CA100183 awarded to Riverside Research and the Riverside Research Fund for Biomedical Engineering Research.

References

[1] M. de Boer, J. A. van Dijck, P. Bult, G. F. Borm, and V. C. Tjan-Heijnen, "Breast cancer prognosis and occult lymph node metastases, isolated tumor cells, and micrometastases," *J Natl Cancer Inst*, vol. 102, no. 6, pp. 410–25, 2010.

[2] M. Hata, J. Machi, J. Mamou, E. T. Yanagihara, E. Saegusa-Beecroft, G. K. Kobayashi, C. C. Wong, C. Fung, E. J. Feleppa, and K. Sakamoto, "Entire-volume serial histological examination for detection of micrometastases in lymph nodes of colorectal cancers," *Pathol Oncol Res*, vol. 17, no. 4, pp. 835–41, 2011.

[3] J. Mamou, A. Coron, M. Hata, J. Machi, E. Yanagihara, P. Laugier, and E. J. Feleppa, "Three-dimensional high-frequency characterization of cancerous lymph nodes," *Ultrasound Med Biol*, vol. 36, pp. 361–375, 2010.

[4] J. Mamou, A. Coron, M. L. Oelze, E. Saegusa-Beecroft, M. Hata, P. Lee, J. Machi, E. Yanagihara, P. Laugier, and E. J. Feleppa, "Three-dimensional high-frequency backscatter and envelope quantification of cancerous human lymph nodes," *Ultrasound Med Biol*, vol. 37, no. 3, pp. 345–57, 2011.

[5] E. Saegusa-Beecroft, J. Machi, J. Mamou, M. Hata, A. Coron, E. Yanagihara, T. Yamaguchi, M. L. Oelze, P. . Lee, P. Laugier, and E. J. Feleppa, "3D quantitative ultrasound for detecting lymph-node metastases," *Journal of Surgical Research*, In Press.

[6] M. L. Oelze, J. F. Zachary, and W. D. O'Brien, Jr., "Characterization of tissue microstructure using ultrasonic backscatter: Theory and technique for optimization using a Gaussian form factor," *J. Acoust. Soc. Am.*, vol. 112, pp. 1202–1211, 2002.

[7] J. Mamou, E. Saegusa-Beecroft, A. Coron, M. L. Oelze, T. Yamaguchi, M. Hata, J. Machi, E. Yanagihara, P. Laugier, and E. J. Feleppa, "Lymph explorer: a new gui using 3d high-frequency quantitative ultrasound methods to guide pathologists towards metastatic regions in human lymph nodes," *Proceedings of the 2012 IEEE Ultrasonics Symposium*, pp. 2340–2343, 2012.